Eckels, S.J., T.M. Doer, and M.B. Pate, *In-tube heat transfer and pressure drop of R-134a and Ester lubricant mixtures in a smooth tube and a micro-fin tube: Part I-Evaporation.* ASHRAE Transaction, 1994. **100**(2): p. 265-282

In-tube Heat Transfer and Pressure Drop of HFC-134a and Ester Lubricant Mixtures in a Smooth Tube and a Micro-Fin Tube: Part I Evaporation

S. J. Eckels
Member ASHRAE
Assistant Professor
Kansas State Unversity

T. M. Doerr
Student Member ASHRAE
Graduate Research Assistant.
Iowa State University

M. B. Pate
Member ASHRAE
Professor
Iowa State University

ABSTRACT

In-tube heat transfer coefficients and pressure drop during evaporation are reported for mixtures of HFC-134a and a penta erythritol ester mixed-acid lubricant. The ester lubricant was tested at viscosities of 169 SUS and 369 SUS over a lubricant concentration range of 0% to 5% in both a smooth tube and micro-fin tube. The average saturation temperature used was 1°C (33.8 °F). Measurements were taken for the refrigerant-lubricant mixture over a mass flux range of 85 kg/m^{2}s (62,700 lb/ft^2 hr) to 375 kg/m^{2}s (276,640 lb/ft^2 hr) in 9.52-mm (3/8 in) outer diameter test tubes.

Heat transfer coefficients during evaporation increased at low concentrations of the 169 SUS ester lubricant and then dropped off at high lubricant concentrations in both the smooth tube and micro-fin tube. The higher viscosity 369 SUS lubricant decreased the heat transfer coefficients in both tubes over the range of lubricant concentrations tested. Pressure drops during evaporation increased in both the smooth tube and micro-fin tube with the addition of either viscosity ester lubricant. The heat transfer coefficients for the micro-fin tube were 100% to 50% higher than those for the smooth tube with the higher values occurring at low mass fluxes. Pressure drops in the micro-fin tube were 10% to 20% higher than those for the smooth tube.

INTRODUCTION

Evaluation of HFC-134a heat transfer coefficients and pressure drops is important as new systems are designed to utilize this alternate refrigerant. This paper is the second in a series of papers reporting the results of ASHRAE research project RP-630. The goal of RP-630 is to expand the current base of HFC-134a heat transfer data to include both smooth and enhanced tubes (i.e., a micro-fin tube). In addition, RP-630 investigates the effect circulating lubricant has on the evaporation performance of HFC-134a. This paper reports in-tube evaporation heat transfer coefficients and pressure drops for mixtures of HFC-134a and a penta erythritol ester mixed-acid lubricant. The heat transfer coefficients and pressure drops reported are averaged over the 3.6-m-long (12 ft.), 9.52 mm (3/8 in) outer diameter smooth tube and micro-fin tube. Condensation results for this mixture, also a part of RP-630, are reported in a companion paper Eckels et al. (1994).

The paper will first review the HFC-134a data currently available in literature. Next, the experimental rig and data analysis equations are discussed. Experimental data for the HFC-134a/ester lubricant mixtures in both the smooth tube and the micro-fin tube are also presented. The performance benefits of the micro-fin tube are also quantified and discussed for HFC-134a.

Finally, design equations are presented for the HFC-134a/ester lubricant mixtures in the smooth tube and micro-fin tube.

LITERATURE REVIEW

Four studies were found that dealt with heat transfer and pressure drop characteristic of-HFC-134a during evaporation. Hambraeus (1991) reported heat transfer coefficients for a HFC-134a/synthetic oil mixture during evaporation. The effect of lubricant concentration was reported to be very dependent on the heat flux applied to the electrically heated 12-mm (0.47 in) outer diameter smooth tube. Below 4 kW/m^2 (1270 BTU/hr ft^2), the heat transfer coefficients increased with the addition of lubricant. Above 6 kW/m^2 (1905 BTU/hr ft^2), the addition of lubricant decreased the heat transfer coefficients.

Eckels and Pate (1991) reported the effect of a 150 SUS polyalkylene glycol (PAG) on the average heat transfer coefficients of HFC-134a during evaporation. The test tube was a 3.66-m-long (12 ft), 9.52-mm (3/8 in) outer diameter smooth tube. Evaporation heat transfer coefficients for the HFC-134a/PAG mixture were increased by about 10% at lubricant concentrations of 1.2% and 2.4%, while at a 5.5% lubricant concentration, the evaporation heat transfer coefficients were about 50% lower than those of the pure refrigerant.

Fukushima and Kudou (1990) studied the effect of a PAG lubricant on the local evaporation heat transfer coefficients and pressure drops of HFC-134a. Evaporation tests were performed in a 1.6-m-long (5.25 ft) by 5.5-mm (0.22 in) outside diameter tube that was heated by direct electrical current. They reported slight increases in the heat transfer coefficients at low qualities over the 0% to 10% lubricant concentration range tested. At the higher qualities, the heat transfer coefficients were shown to always degrade with the addition of lubricant. At a 10% lubricant concentration, average heat transfer coefficients for the test section were decreased by 10% over the pure refrigerant results. Evaporation pressure drops for HFC-134a were shown to increase linearly with lubricant concentration with approximately a 120% increase at a 10% lubricant concentration.

Torikoshi and Kawabata (1992) reported average evaporation heat transfer coefficients and pressure drops for HFC-134a/PAG lubricant mixtures in a smooth tube and a micro-fin tube. In the 9.52-mm (3/8 in) outside diameter smooth tube and micro-fin tube, the addition of lubricant increased the evaporation heat transfer coefficients at low lubricant concentration, while at high lubricant concentrations the heat transfer coefficients were degraded. The micro-fin tube heat transfer coefficients were reported to be about 100% higher than those for the smooth tube over the 50 kg/m^{2}s (36,885 lb/ft^2 h) to 200 kg/m^{2}s (147,540 lb/ft^2 h) mass flux range tested. Evaporation pressure drops for the micro-fin tube were reported to be slightly higher than those for the smooth tube.

TEST FACILITIES

The test rig is composed of five main sections: the test section, the refrigerant loop, the water loop, the water-glycol loop, and the oil charging station. The test facility measures the in-tube average heat transfer coefficients and pressure drops of a pure refrigerant or a refrigerant-lubricant mixture over the length of a test tube. A schematic diagram of the test facility is shown in Figure 1. In the following paragraphs, each of the five main sections of the rig is described.

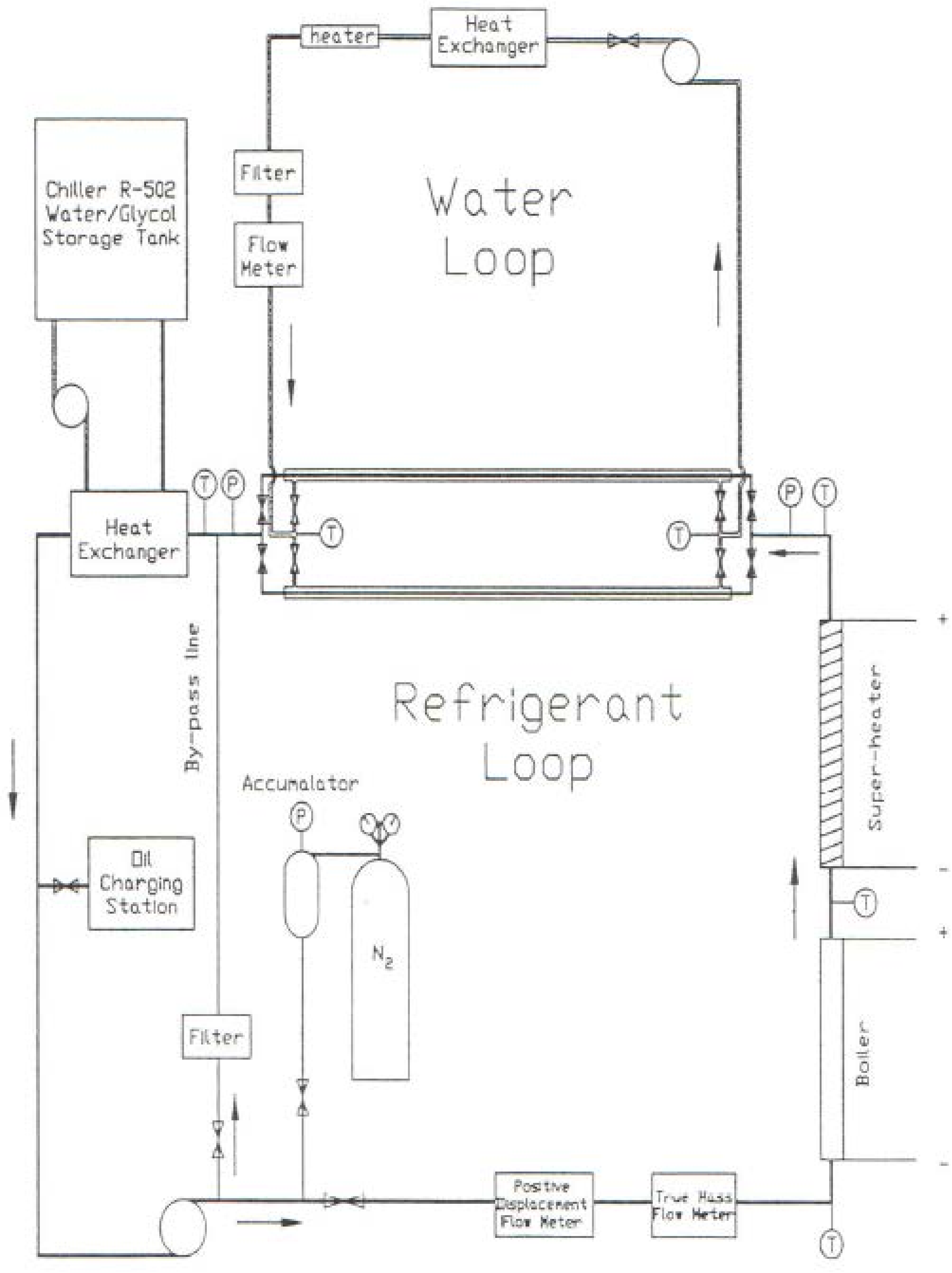

Figure 1: Schematic Diagram of test facility

<u>Test Section</u>

The test section consists of two tube-in-tube heat exchangers, temperature sensors, pressure sensors, and routing valves. The test section contains two identical tube-in-tube counter flow heat exchangers which are mounted parallel. A different test tube is mounted in each heat exchanger. During testing only one of the heat exchangers is active, the other heat exchanger isisolated with a series of valves. The inner tube of the heat exchanger (i.e., the micro-fin tube or smooth tube) is a 9.52-mm (3/8 in) outer diameter tube which is 3.67-m (12 ft) in length. The outer tube of the heat exchanger is also 3.67-m (12 ft) long with a 17.2-mm (0.67 in) inner diameter. Refrigerant flows in the inner tube and water in the outer annulus. The water flowing in the outer tube is used to either vaporize or condense the refrigerant flowing in the inner tube.

Temperatures of the inlet and outlet streams of either heat exchanger in the test section are measured with resistance temperature devices (RTDs) which have a manufacturers uncertainty of $\pm$0.05 ^{o}C (0.09 ^{o}F). The pressure at the inlet of the refrigerant tube is measured by two pressure transducers: a capacitance sensing transducer with an uncertainty of $\pm$2.1 kPa (0.3 PSI) and a strain gauge type transducer with an uncertainty of $\pm$9 kPa (1.3 PSI). The pressure drop across the refrigerant test tube is measured with a capacitance sensing type differential pressure transducer accurate to $\pm$0.17 kPa (0.025 PSI).

Refrigerant Loop

The refrigerant loop contains an after condenser, a positive displacement pump, a bladder accumulator, a filter drier, two flow meters, a boiler, and instrumentation. The refrigerant loop does not use a compressor, rather a positive displacement pump is used to circulate the refrigerant. The advantage of the positive displacement pump is that it does not require lubrication during operation and hence, lubricant concentration can be a parameter of the system.

The refrigerant exiting the test section is condensed and subcooled in the after-condenser. The subcooled refrigerant is then circulated with the positive displacement pump which produces a constant volume flow of liquid refrigerant. The flow rate of refrigerant into the test section is controlled with a by-pass line that diverts a certain portion of the flow away from the test section. Prior to entering the test section, the refrigerant is heated to the proper temperature and quality in the boiler. The boiler is a 12.7-mm (1/2 in) outer diameter, 2.63-m (8.6 ft) long stainless-steel tube heated by direct electrical current. The pressure in the refrigerant line is controlled with the bladder accumulator that acts as an expansion tank.

The refrigerant flow rate into the test section is measured by two flow meters: a coriolis effect flow meter and a positive displacement flow meter. The two flow meters are mounted in series directly before the test section and boiler. The coriolis effect flow meter has an accuracy of $\pm$0.15%, while the positive displacement flow meter has an accuracy of $\pm$1.0%. The coriolis effect flow meter measurements were used in the data analysis. Temperatures in the refrigerant line are monitored in various locations with thermocouples, accurate to +0.3 ^{o}C. The temperature of the refrigerant entering and exiting the test section is measured with RTDs, accurate to $\pm$0.05 ^{o}C (0.09 ^{o}F).

Water Loop

Water entering the annulus side of the heat exchangers in the test section is supplied by the water loop. The water loop contains a pump, a heater, a heat exchanger, and a coriolis effect flow meter. A pump circulates the water in the loop, with flow control provided by a globe valve. The water is then passed through the heat exchanger and heater where energy is added or removed depending on the type of test being conducted in the test section (i.e., condensation or evaporation). The flow rate of the water is measured with a coriolis effect flow meter which is accurate to $\pm$0.15%. The temperature of the water entering and exiting the test section ismeasured with RTDs, accurate to $\pm$0.05 ºC (0.09 ºF).

Water-Glycol Loop

The water-glycol loop supplies the medium used to condense the refrigerant exiting the test section. Water-glycol is circulated through the after-condenser in the refrigerant line with the water-glycol pump. The pump is fed from a 1137 L (300 gallon) storage tank that is cooled to -15 ºC (5 ºF) with a 105 kW (30 ton) nominal chiller.

Oil Charging Station

Lubricant is injected into the refrigerant line with a pneumatic cylinder, which is a double-actuating cylinder with a 5.1 cm (2 in) diameter and a 15.2 cm (6 in) stroke. High pressure nitrogen is used on the opposing side of the lubricant charge to drive the lubricant into the refrigerant line. The amount of lubricant injected into the system is calibrated to the volume displacement of the charging cylinder, thus allowing an accurate charge to be injected.

A second pneumatic cylinder with a 3.17 cm (1.25 in) diameter and a 10.16 cm (4 in) stroke is used to draw samples from the refrigerant line in order to verify the flowing lubricant concentration. The lubricant concentration of the refrigerant/lubricant mixture in the sampling cylinder is determined by knowing the weight of the cylinder empty, the weight of the cylinder and the refrigerant/lubricant mixture, and the weight after the refrigerant has been bled off. The cylinder system was weighed at each step with an electronic scale accurate to $\pm$0.01 g. ASHRAE standard 41.-4-1984 (1984a) was used to calculate the reported lubricant concentrations. The sampling sizes used in this study were smaller than those recommended in ASHRAE Standard 41.4-1984 due to volume limitations of the test facility.

DATA REDUCTION

The average convective heat transfer coefficients in the test tube are determined by a log-mean-temperature-difference (LMTD) method. Two categories of experimental data must be analyzed: pure refrigerant data and refrigerant/lubricant mixture data. For pure refrigerants, application of the data reduction equations is straightforward, but when refrigerant/lubricant mixtures are being analyzed a few modifications to the data reduction equations are necessary. In the following paragraphs, the pure refrigerant data reduction equations are presented. The adjustments to the data reduction equations necessary when analyzing refrigerant/lubricant mixtures are discussed in the next section. Finally, the experimental uncertainties associated with the data are given.

Pure Refrigerant

The energy transferred to the refrigerant in the test section during two-phase flow and single-phase flow is calculated from an energy balance on the water-side of the test section.

$$Q_{TW} = m_w c_{pw}(T_I - T_O) \tag{1}$$

During single-phase flow, an energy balance can also be applied to the refrigerant flowing through the test section.

$$Q_{Tr} = m_r c_{pr}(T_I - T_O) \tag{2}$$

Comparisons of the water-side energy balance and refrigerant-side energy balance during single-phase flows showed that the two are in good agreement--within $\pm$3%.

The quality entering the test section is determined by applying an energy balance to the preheaters. The energy transfer to the refrigerant in the preheater is calculated from the the enthalpy leaving and entering the preheater. The enthalpy leaving the preheater is given by.

$$H_O = m_r c_{pr}\left(T_{sat} - T_{ref}\right) + m_r i_{fg} x \tag{3}$$

where T_{ref} is some arbitrary reference temperature. The refrigerant entering the preheater is always subcooled so the enthalpy entering is

$$H_I = m_r c_{pr}\left(T_{hi} - T_{ref}\right) + m_r i_{fg} x \tag{4}$$

The energy input by the preheater is calculated by measuring the voltage and current across the heater. The equation used to determine the energy input to the refrigerant in the pre-heater is

$$Q_h = HL1(V \cdot I) + HL2 \tag{5}$$

where factors HL1 and HL2 account for the energy gained or lost to the environment during testing (Schlager 1989). During evaporation, HL1 is 1 and HL2 is 80 W. Substituting the known values into an energy balance and solving for quality exiting the preheater gives.

$$x = \frac{1}{i_{fg}}\left(\frac{HL1(V \cdot I) + HL2}{m_r} - c_{pr}\left(T_{sat} - T_{ref}\right)\right) \tag{6}$$

The quality change through the test section is determined in a similar manner using the refrigerant enthalpies entering and exiting the test section. The resulting formula for the quality change across the test section is

$$\Delta x = \frac{Q_{T_w}}{m_r i_{fg}} \tag{7}$$

Equations 6 and 7 are sufficient to determine the qualities in the refrigerant line as long as subcooled liquid enters the preheater and the superheat vapor region is not entered.

The average heat transfer coefficient of the refrigerant in the test tube is determined from the overall heat transfer coefficient, the annulus-side heat transfer coefficient, and the LMTD. The overall heat transfer coefficient is

$$U_o = \frac{Q_{T_w}}{LMTD \cdot a_o} \tag{8}$$

The log-mean-temperature-difference is determined from the temperatures at the inlet and exit of annulus-side of the heat exchanger and the average saturation temperature of the refrigerant in the inner tube. The average saturation temperature of the refrigerant is inferred from the average saturation pressure in the tube. The annulus-side heat transfer coefficient h_o was correlated with a Wilson-plot technique over the range of flow rates and temperatures typically encountered in the annulus during testing. The average in-tube heat transfer coefficient can be calculated by forming a simple resistance network. Assuming that the resistance of the copper tube is negligible, and solving for inside heat transfer coefficient gives.

$$h_i = \frac{1}{\left(\frac{1}{U_o} - \frac{1}{h_o}\right)\frac{a_i}{a_o}} \tag{9}$$

The inside surface area (a_i) is based on the maximum inside diameter of the smooth tube and micro-fin tube. The maximum inside diameter for the micro-fin tube is defined as the outer diameter of the micro-fin tube minus twice the minimum wall thickness. For the tubes used in this study, the smooth tube had a maximum inside diameter of 8.0 mm (0.315 in) and the micro-fin tube had a 8.92 mm (0.351 in) maximum inside diameter.

Data Reduction with Refrigerant-Lubricant Mixtures

Adjustments to the data reduction equations are necessary to account for the presence of refrigerant/lubricant mixtures. The specific heat of the refrigerant used in Equations 2,4 and 6 must be adjusted to account for the presence of lubricant. The mixing equation used to determine the specific heat of a refrigerant/lubricant mixture is (Jensen and Jackman 1984):

$$c_{pm} = c_{pr}\omega_r + c_{pl}(1 - \omega_r) \tag{10}$$

The density of the refrigerant/lubricant mixture is also required. Specifically, the positive displacement flow meter, which is used as a backup flow meter, requires a density to convert volumetric flow to mass flow. The mixing equation used to determine the density of a refrigerant/lubricant mixture is (ASHRAE 1984b):

$$\rho_m = \frac{\rho_r}{1 - (1 - \omega_r)\left(1 - {}^{\rho_r}/_{\rho_l}\right)} \tag{11}$$

The LMTD used in Equation 8 requires the average saturation temperature of the refrigerant in the test section. For a pure refrigerant, the average pressure in the refrigerant tube is used to determine the average saturation temperature. If a refrigerant/lubricant mixture is present, solubility data must be used to determine the average temperature in the test section. Specifically, calculating an average saturation temperature for pure refrigerant only requires an accurate relationship between P_{sat} and T_{sat}, whereas with a refrigerant/lubricant mixture an accurate relationship between P_{sat}, T_{sat}, and lubricant concentration (i.e., solubility data) must be known. The data acquisition system records both the pressure and temperature information for the refrigerant in the test section but only the pressure measurements are used in determining the saturation temperature. A detailed description of the experimental facility used to obtain solubility data for the refrigerant/lubricant mixtures and the methodology used in determining the average saturation temperature in the test section were given in Eckels et al. (1993).

Experimental Uncertainties

The uncertainties in the average heat transfer coefficients and pressure drops of pure HFC-134a were calculated from a sample of the pure HFC-134a test runs in the smooth tube and the micro-fin tube. A propagation-of-error analysis (Kline and McClintock 1953) was used to obtain the uncertainty in the average heat transfer coefficient, while a statistical method was used to determine the uncertainty in pressure drop. The uncertainties for the smooth tube are listed in Table 1, while the uncertainties in the micro-fin tube data are listed in Table 2. The uncertainties listed for pressure drop are a 95% confidence interval on the mean pressure drop calculated in each test run. The uncertainties shown above are only for pure HFC-134a. The uncertainties in the average heat transfer coefficient for refrigerant/lubricant mixtures can be calculated by including the uncertainties in LMTD caused the refrigerant/lubricant mixture. Eckels et al (1993) showed that solubility data for the refrigerant/lubricant mixtures used in this study could be used to accurately predict temperatures measured in an evaporator.

Table 1: Error analysis of smooth tube results

Mass Flux Kg/m² s	Heat Transfer coefficient W/m² K	Quality in %	Quality out %	Pressure drop kPa
86 ±1.7	1694 ±165	5 ±3	85 ±8	2.15 ±0.24
121 ±2.5	2353 ±209	5 ±3	82 ±5	4.66 ±0.42
200 ±4.0	3459 ±295	11 ±3	82 ±5	13.35 ±0.74
310 ±6.2	4485 ±324	7 ±3	82 ±5	27.40 ±0.82
362 ±7.3	5238 ±394	11 ±3	83 ±4	38.72 ±0.78

Table 2: Error analysis of micro-fin tube results

Mass Flux kg/m² s	Heat transfer coefficient W/m² K	Quality in %	Quality out %	Pressure drop kPa
85 ±1.6	3812 ±662	8 ±3	84 ±7	3.33 ±0.23
129 ±2.4	4851 ±717	5 ±3	82 ±6	5.55 ±0.59
286 ±5.4	6861 ±795	8 ±3	80 ±4	27.22 ±1.04
367 ±6.9	7513 ±777	7 ±3	82 ±4	40.06 ±1.20

EXPERIMENTAL RESULTS

In-tube heat transfer coefficients and pressure drops during evaporation are presented for mixtures of HFC-134a and a penta erythritol ester mixed-acid lubricant. The test tubes were a 9.52-mm (3/8 in) outer diameter smooth tube and micro-fin tube. The ester lubricant was tested at viscosity levels of 169 SUS and 369 SUS. For the 169-SUS ester lubricant, lubricant concentrations of 0.5%, 1.0%, 1.9%, 2.9%, and 5.0% were used, while for the 369-SUS ester lubricant, the lubricant concentrations used were 0.6%, 1.1%, 2.4%, 5.0%. The range of conditions used during testing is shown in Table 3. The dimensions of the smooth tube and micro-fin tube are listed in Table 4.

The heat transfer coefficients in the smooth tube and the micro-fin tube are discussed first. Next, the results for evaporation pressure drops are discussed. For each series of tests, the effect of lubricant concentration is quantified by forming heat transfer enhancement factors ($EF_{s'/s}$ or $EF_{a'/a}$) or pressure drop penalty factors ($PF_{s'/s}$ or $PF_{a'/a}$). The subscripts denote which ratio is being formed. For example, the "a" subscript represents augmented tube and "a'" the augmented tube with lubricant added. The subscript s is used for smooth tube results. The EFs'/s ratio would represent the heat transfer coefficient of refrigerant/lubricant mixture in the smooth tube divided by the pure refrigerant heat transfer coefficient in the smooth tube. A direct comparison of the smooth tube results and the micro-fin tube results are presented in the next section.

Table 3: Test conditions

	Smooth tube & Micro-fin tube
Temperature (°C)	1
Pressure (MPa)	0.35
Mass flux (kg/m^2 s)	85 - 375
Quality in (%)	5 - 10
Quality out (%)	80 - 88
Lubricant Concentration (%)	0 - 5

Table 4: Micro-fin tube and smooth tube dimensions

	Micro-fin tube	Smooth tube
Outside Diameter, mm	9.52	9.52
Wall Thickness , mm	0.3	0.76
Maximum inside diameter, mm	8.92	8
Cross section area, mm^2	58.1	50.3
Fin height, mm	0.2	--
Spiral Angle, °	17	--
Number of fins	60	--

Heat Transfer

Heat transfer coefficients during evaporation of the HFC-134a/169 SUS ester lubricant mixture in both the smooth tube and the micro-fin tube are shown in Figure 2. The lines shown on the figure are a least squares curve fit of the data at each lubricant concentration. Figure 3 presents the heat transfer coefficients for mixtures of HFC-134a and the 369 SUS ester lubricant. Figure 4 presents the heat transfer enhancement factor $EF_{s'/s}$ for both refrigerant/lubricant mixtures in the smooth tube. The least square lines shown on Figures 2 and 3 for the smooth tube were used to form the $EF_{s'/s}$ ratio. Figure 4 shows that the viscosity of the lubricant does have a significant effect on the performance of the refrigerant/lubricant mixture in the smooth tube. For the 169 SUS ester lubricant, the maximum $EF_{s'/s}$ value is about 1.1 and occurs at a 1.9% lubricant concentration, while the minimum $EF_{s'/s}$ value is about 0.75 at a 5% lubricant concentration. The $EF_{s'/s}$ ratio for the 369 SUS ester lubricant continually decreases with lubricant concentration to values of about 0.72 at a 5% lubricant concentration.

The $EF_{a'/a}$ ratio for the micro-fin tube is shown in Figure 5. The ratio is formed from the micro-fin tube results presented in Figures 2 and 3. The $EF_{a'/a}$ ratio shows that lubricant viscosity also has a significant effect on the micro-fin tube performance. The 169 SUS ester lubricant had $EF_{a'/a}$ ratios larger than 1.0 over the range of lubricant concentrations tested. The higher viscosity 369 SUS ester lubricant shows a degraded $EF_{a'/a}$ ratio for all lubricant concentrations tested.

The evaporation heat transfer coefficients of pure HFC-134a in the smooth tube are compared with correlations of Shah (1982), Kandlikar (1987), Chaddock-Brunemann (1967), Gungor-Winterton (1986), and Jung et al. (1989). Figure 6 compares the experimentally determined heat transfer coefficients with the predicted heat transfer coefficients. The figure shows that the experimental heat transfer coefficients were predicted within $\pm$20% by all correlations except the Gungor-Winterton correlation. The Kandlikar and Jung-Radermacher correlations give the best estimate of the experimental data.

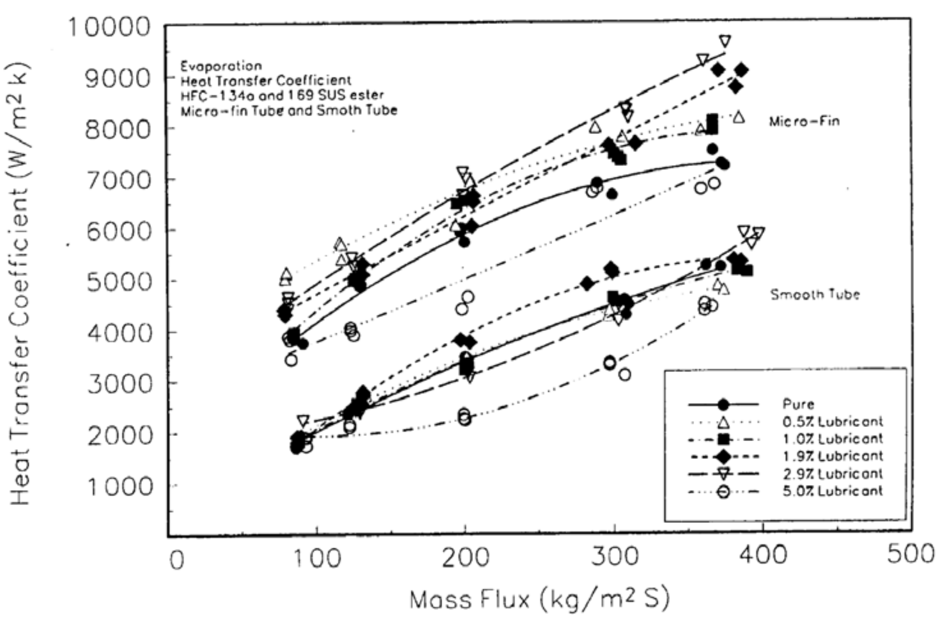

Figure 2: Evaporation heat transfer coefficient for mixtures of R-134a adn 169-SUS ester Lubricant in a micro-fin tube and a smooth tube

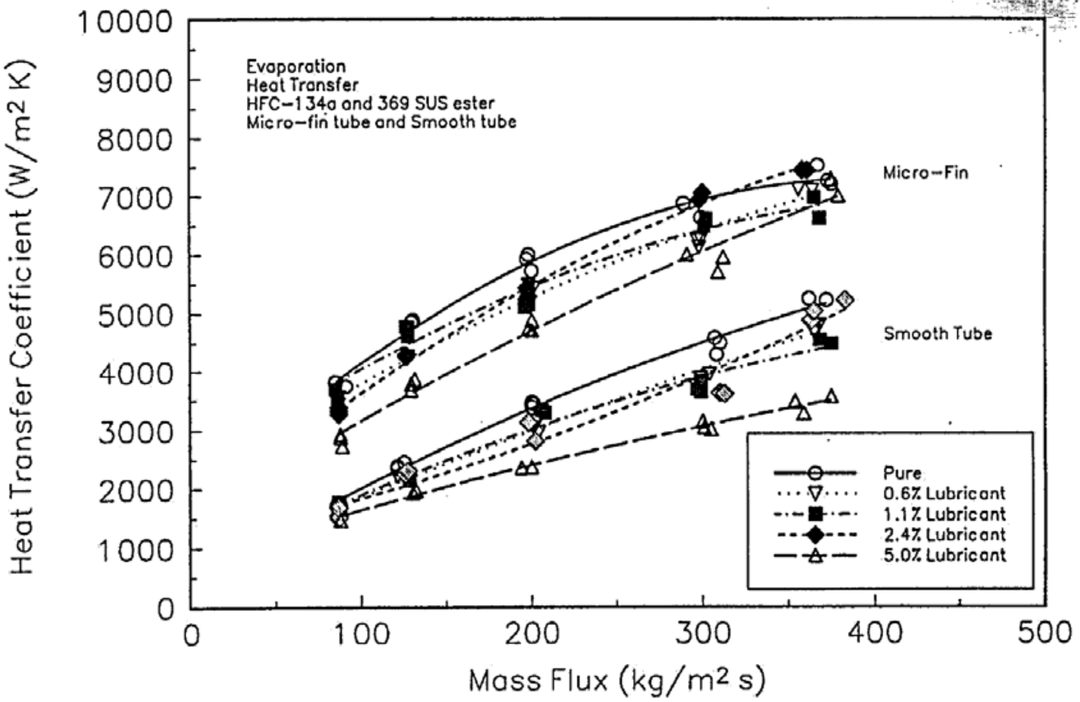

Figure 3: Evaporation heat transfer coefficients for mixtures of HFC-134a and 369SUS ester

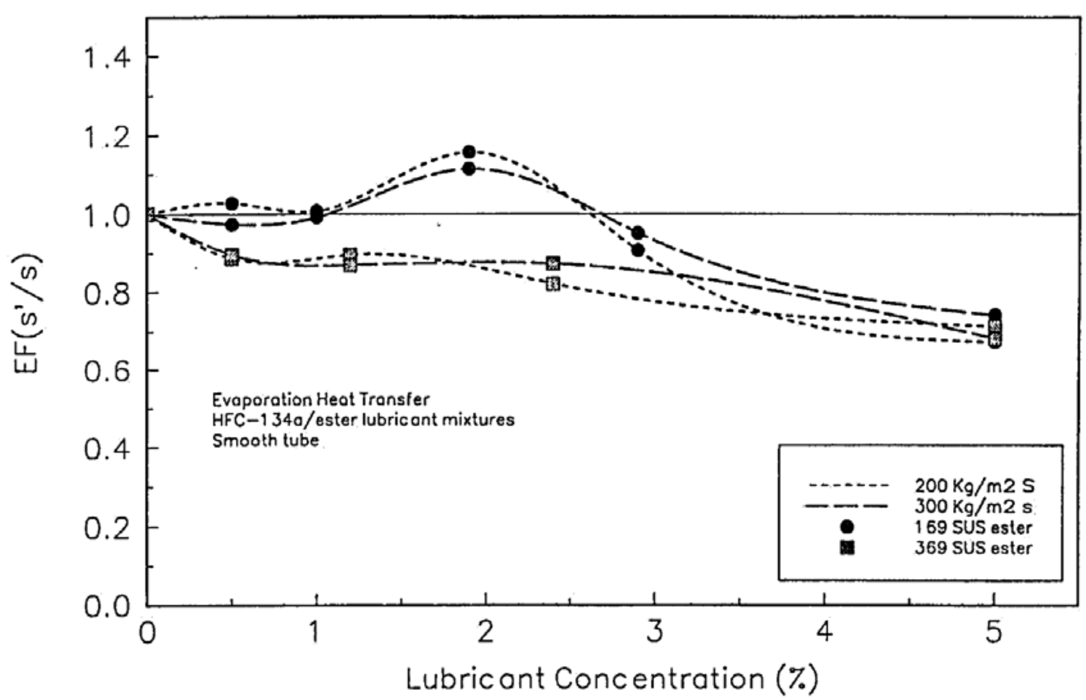

Figure 4: Heat transfer enhancement factors for HFC-134a/ester lubricant mixtures in the smooth tube.

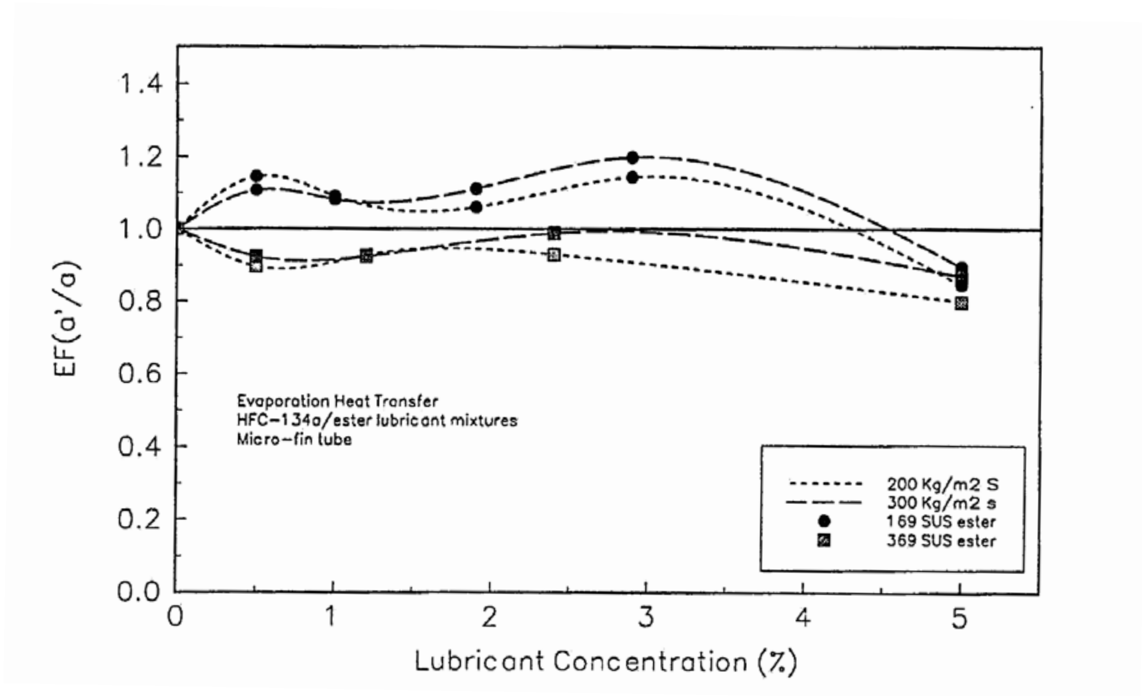

Figure 5: Heat transfer enhancement factors for HFC-134a/ester lubricant mixtures in the micro-fin tube.

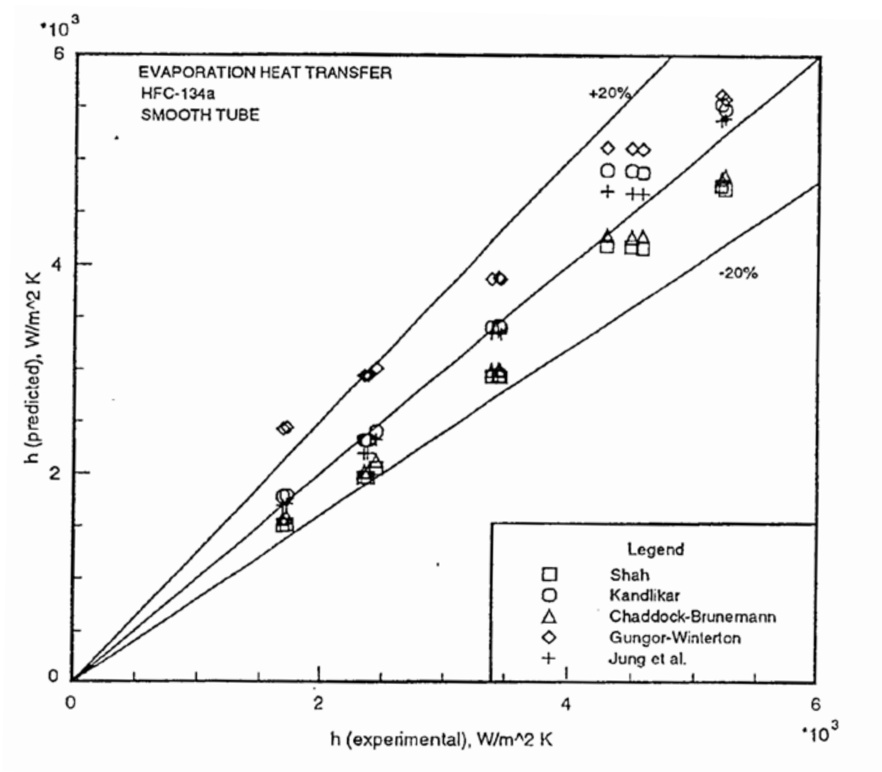

Figure 6: Comparison of evaporation heat transfer coefficients for pure HFC-134a with predicted values.

Pressure Drop

Figure 7 presents evaporation pressure drops in the smooth tube and the micro-fin tube for the HFC-134a/169 SUS ester mixture. Only two lubricant concentrations have been included in the figure, although data were obtained at all lubricant concentrations tested. The figure shows that pressure drop increases with mass flux and lubricant concentration in both the smooth tube and micro-fin tube. Pressure drops for the HFC-134a/369 SUS ester mixture in the smooth tube and the micro-fin tube are shown in Figure 8. The higher viscosity lubricant also shows increased pressure drop with mass flux and lubricant concentration.

The $PF_{s'/s}$ ratio for the smooth tube is presented in Figure 9. The $PF_{s'/s}$ ratio increases with lubricant concentration for both lubricant mixtures. For example, at a 5% lubricant concentration and a mass flux of 200 kg/m^2 s (147,500 lb/ft^2 hr), the $PF_{s'/s}$ ratio is about 1.5 for the 169 SUS ester and about 1.6 for the 369 SUS ester. The $PF_{s'/s}$ ratio at a mass flux of 300 kg/m^{2}s (221,300 lb/ft^2 hr) is generally 10% to 20% lower than the $PF_{s'/s}$ ratio at a mass flux of 200 kg/m^{2}s (147,500 lb/ft$_2$ hr).

Figure 10 shows the $PF_{a'/a}$ ratio for the two ester lubricants in the micro-fin tube. The $PF_{a'/a}$ ratio increases with lubricant concentration over the range of lubricant concentrations tested. The increase appears to be independent of the lubricant concentration or the mass flux of the refrigerant. It is also interesting to note that the increase appears to be less severe than that for the smooth tube.

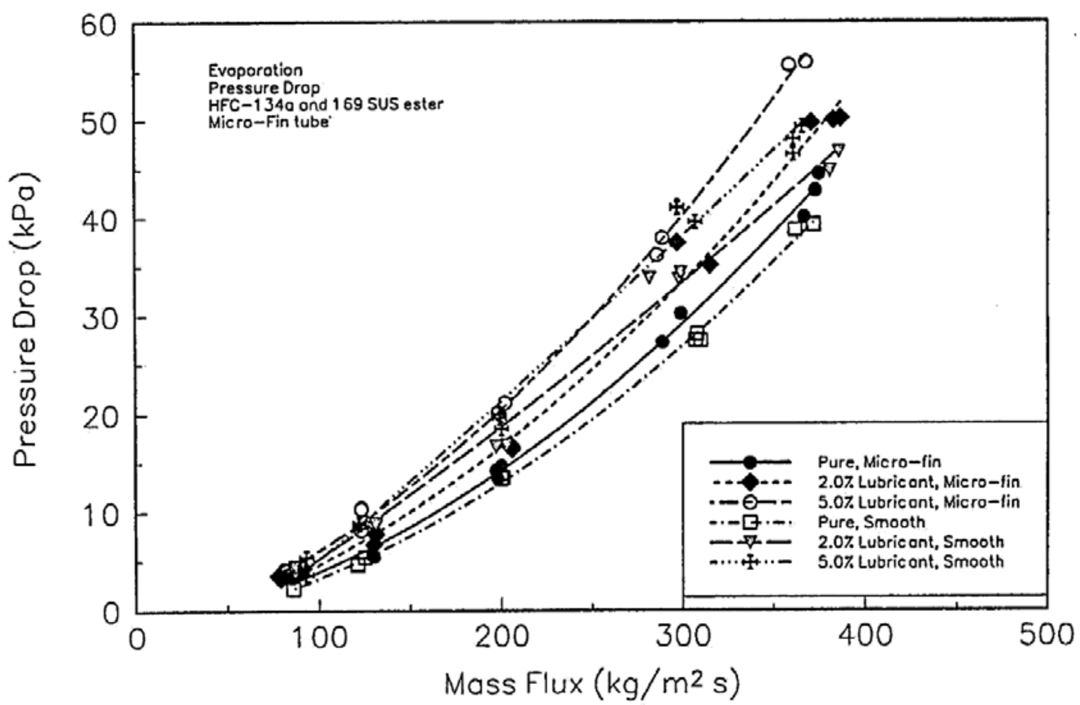

Figure 7: Evaporation pressure drops for mixtures of HFC-134a and 169 SUS ester lubricant in a micro-fin tube and smooth tube.

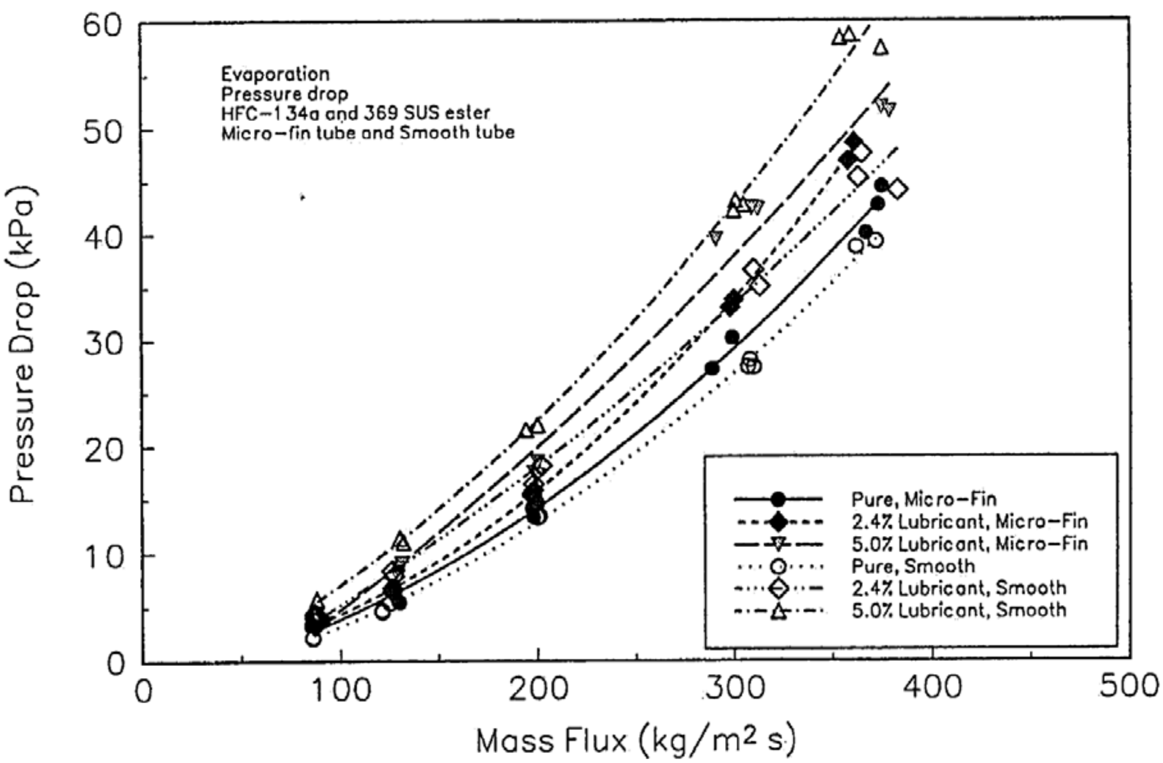

Figure 8: Evaporation pressure drops for mixtures of HFC-134a and 369 SUS ester lubricant in a micro-fin tube and a smooth tube.

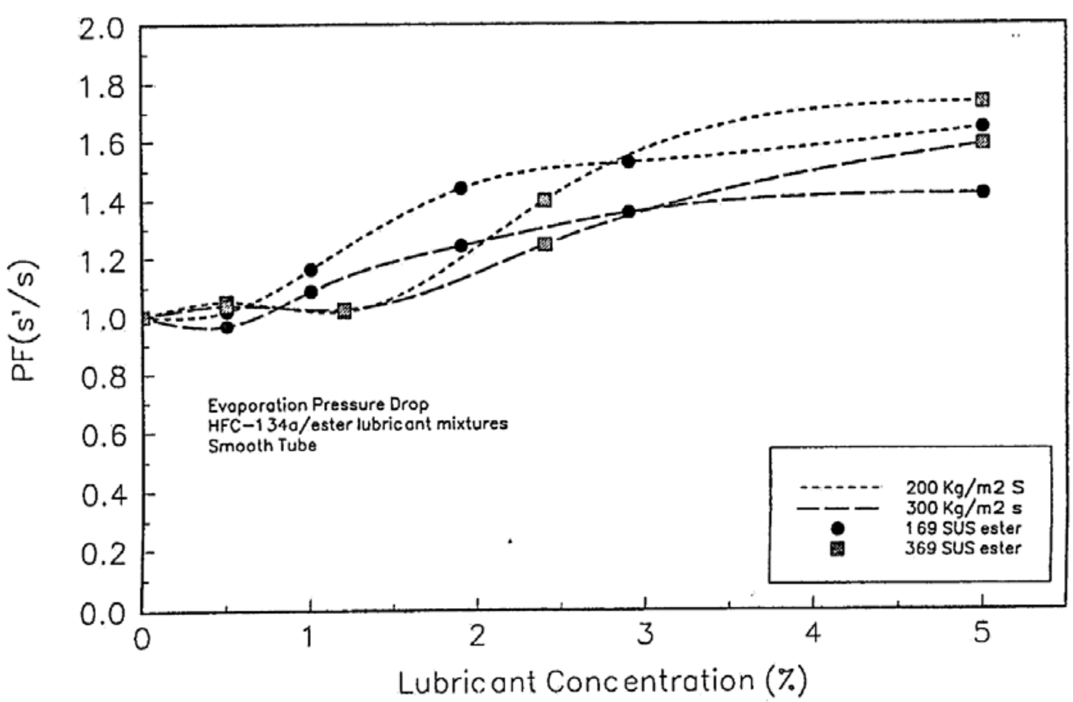

Figure 9: Pressure drop penalty factors for HFC-134a/ester mixtures in the smooth tube

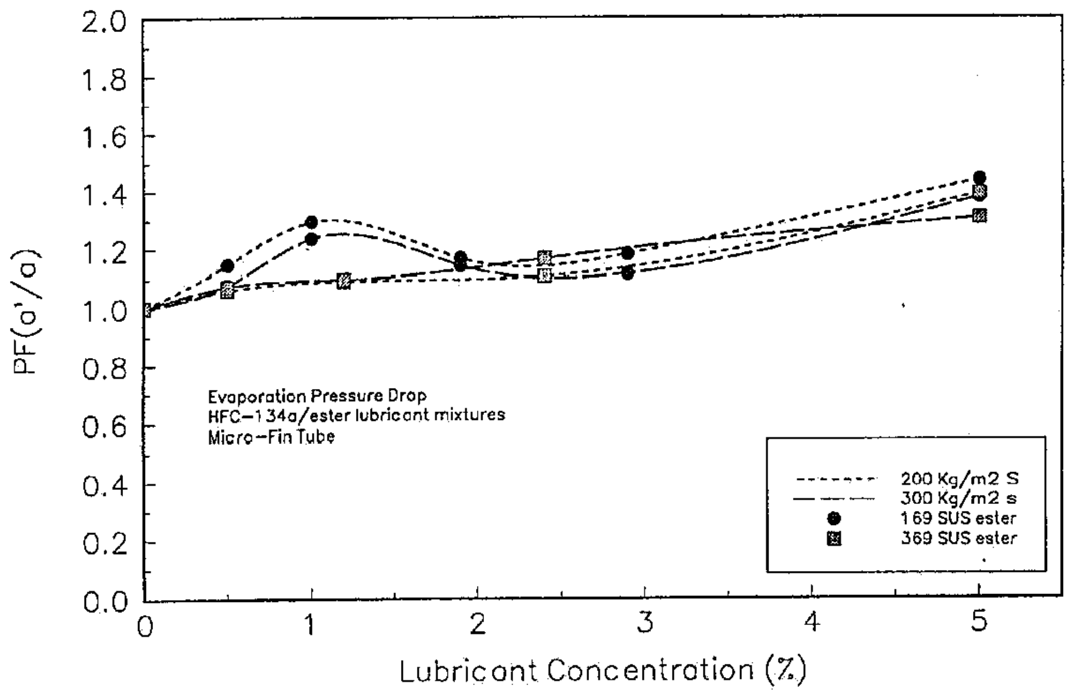

Figure 10: Pressure drop penalty factors for HFC-134a/ester mixtures in the micro-fin tube

COMPARISON OF SMOOTH TUBE AND MICRO-FIN TUBE

The performance benefits of the micro-fin tube are well documented in literature for refrigerant HCFC-22 (Schlager et al. 1987). In this section, the performance benefits of micro-fin tube with refrigerant HFC-134a are evaluated. Specifically, the performance of the micro-fin tube and smooth tube is compared with heat transfer enhancement factors (EF) and pressure drop penalty factors (PF). The pure refrigerant heat transfer enhancement factors ($EF_{a/s}$) and pressure drop penalty factors ($PF_{a/s}$) are presented first. The $EF_{a/s}$ or $PF_{a/s}$ ratio is formed by dividing the pure refrigerant result in the micro-fin tube by the pure refrigerant result in the smooth tube at the same mass flux. The effect of lubricant concentration is also discussed by presenting the $EF_{a'/s'}$ ratio and the $PF_{a'/s'}$ ratio. The $EF_{a'/s'}$ or $PF_{a'/s'}$ ratio is formed by dividing the refrigerant/lubricant mixture results in the micro-fin tube by the refrigerant/lubricant mixture results in the smooth tube at the same mass flux and lubricant concentration. An additional note should be made about the heat transfer enhancement factors when directly comparing the smooth tube and the micro-fin tube. Since the heat transfer coefficients for the micro-fin tube are based on an equivalent smooth tube diameter, the average heat transfer coefficient incorporates the increase in area caused by the addition of fins. The actual surface area of the micro-fin tube used in this study is 1.5 times larger than the equivalent smooth tube surface area used in the calculation of the average heat transfer coefficient.

Pure Refrigerant

The heat transfer enhancement factors ($EF_{a/s}$) and pressure drop penalty factors ($PF_{a/s}$) for pure HFC-134a are shown in Figure 11. The $EF_{a/s}$ ratio ranges from 1.9 at a mass flux of 130 kg/m^{2}s (95,900 lb/ft^2 hr) to 1.5 at a mass flux of 360 kg/m^{2}s (265,600 lb/ft^2 hr), while the

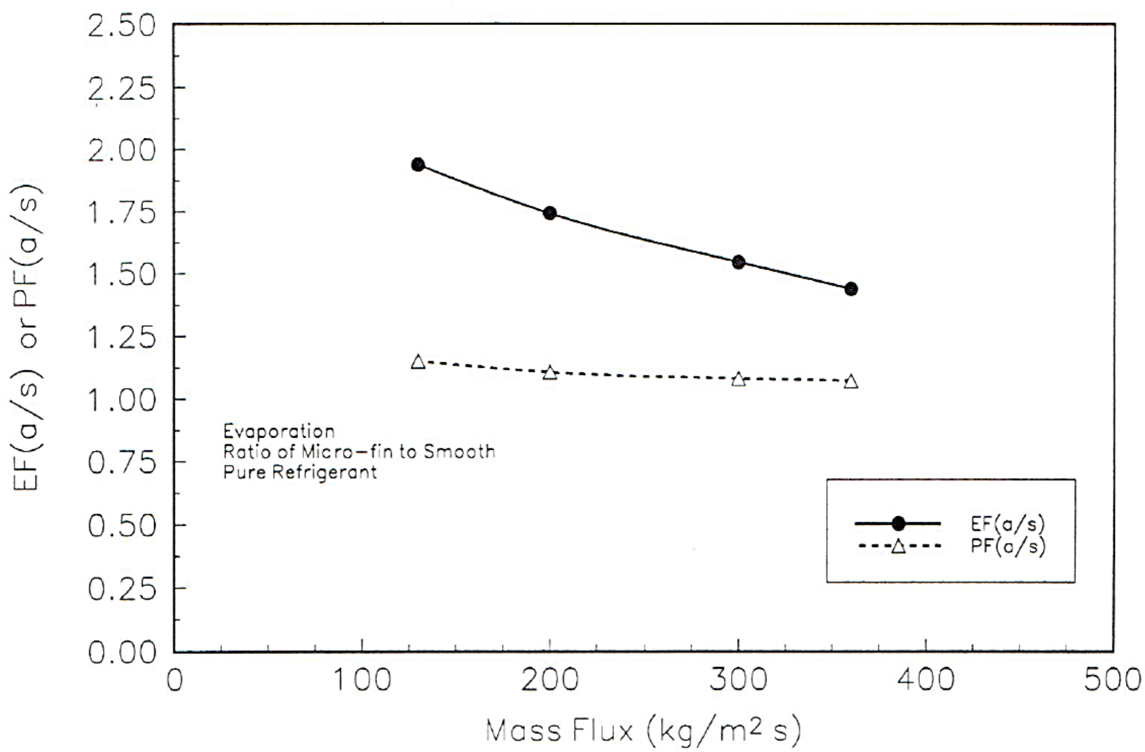

Figure 11: Performance ratios for pure HFC-134a comparing micro-fin tube and smooth tube

pressure drop penalty factor $PF_{a/s}$ ranges from 1.15 to 1.05 over the same mass flux range. These results confirm the performance benefits of the micro-fin tube for pure HFC-134a. Specifically, the heat transfer coefficients are increased by a significant amount with only minimal increases in pressure drop.

<u>Effect of Lubricant Concentration</u>

The effects of lubricant concentration on the performance comparisons of the micro-fin tube and smooth tube are shown by plotting the $EF_{a'/s'}$ and $P_{Fa'/s'}$ ratios versus lubricant concentration. Figure 12 shows the $EF_{a'/s'}$ and $PF_{a'/s'}$ ratios at mass fluxes of 200 kg/m^{2}s (147,500 lb/ft^2 hr) and 300 kg/m^{2}s (221,300 lb/ft^2 hr) for both refrigerant/lubricant mixtures. The lines shown on the graphs are spline fitted to all the data points. The heat transfer enhancement factors $EF_{a'/s'}$ are the upper set of curves on Figure 12. The objective is to identify any trends in the $EF_{a'/s'}$ ratio with lubricant concentration. The $EF_{a'/s'}$ data for both viscosity lubricants and mass fluxes increase with lubricant concentration, indicating that the overall heat transfer performance of the micro-fin tube increases relative to the smooth tube with lubricant concentration.

Evaporation pressure drop penalty factors ($PF_{a'/s'}$) for both viscosity lubricants are also shown in Figure 12. The $PF_{a'/s'}$ ratio increases slightly with lubricant concentration at the 0% to 1.2% range. Beyond a 1.2% lubricant concentration, the $PF_{a'/s'}$ ratio decreases with lubricant concentration. The results shown above indicate that the addition of lubricant in general enhances the heat transfer and pressure drop performance of the micro-fin tube relative to the smooth tube.

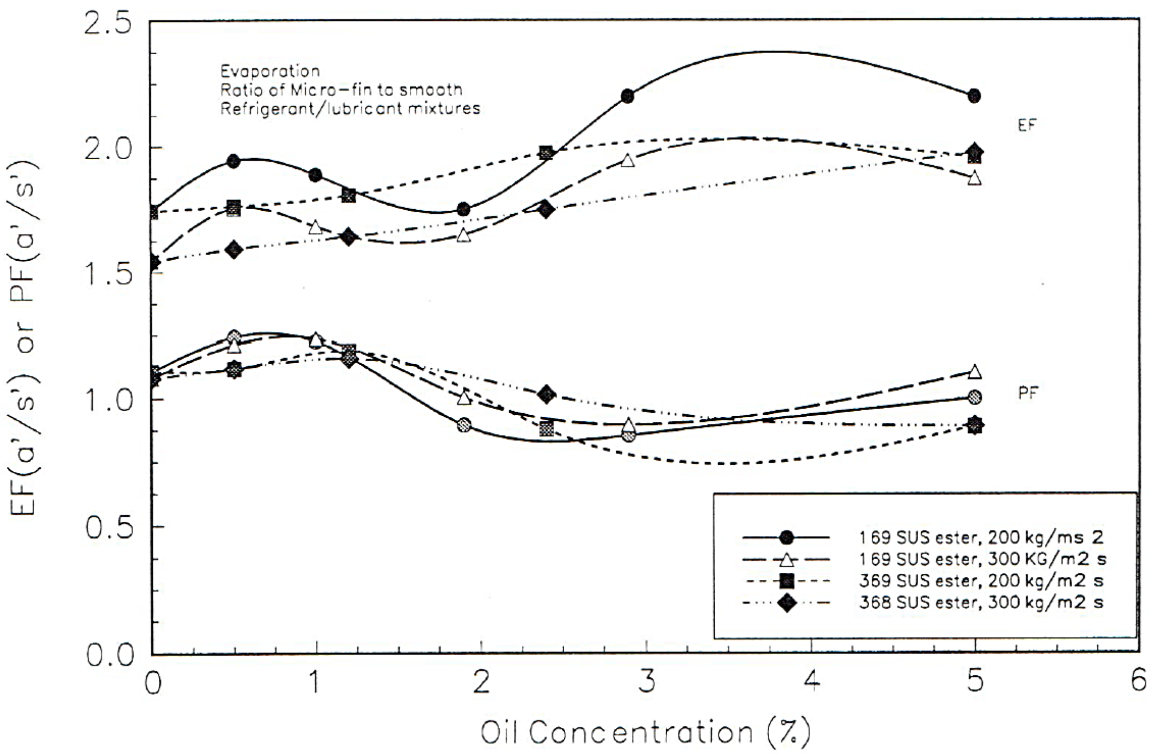

Figure 12: Performance ratios for HFC-134a/ester lubricant mixtures comparing micro-fin tube

DESIGN EQUATIONS

The objective of this section is to present equations that can be used by system designers to model the performance of HFC-134a/ester lubricant mixtures in smooth tubes and micro-fin tubes. The correlations presented in this section are curve fits of the heat transfer enhancement factors and pressure drop penalty factors for the smooth tube and micro-fin tube. For the smooth tube, $EF_{s'/s}$ and $PF_{s'/s}$ ratios were curve fit, while for the micro-fin tube curve fits of the $EF_{a'/s}$ and $PF_{a'/s}$ ratio were used. The design equations should not be extended outside the range of conditions used in this study. The design equations are intended for the specific micro-fin tube and flow conditions used in this study. Application of these design equations is accomplished as follows. Pure refrigerant results in the smooth tube are multiplied by the appropriate heat transfer enhancement factor or pressure drop penalty factor to obtain the desired heat transfer coefficient. For example, if the heat transfer coefficient of a refrigerant-lubricant mixture in the smooth tube is required the following formula would be used:

$$h_{oil} = h_{pure} \cdot EF_{s'/s} \tag{12}$$

The h_{pure} is an appropriate pure refrigerant heat transfer coefficient in the smooth tube, which can be calculated by using any of the several correlations mentioned earlier.

Form of the Correlations

The form of the correlations used to fit the experimentally determined heat transfer enhancement factors and pressure drop penalty factors were empirical in nature. Lubricant mass fraction and refrigerant mass flux were identified as the primary variables effecting the heat transfer enhancement factors and pressure drop penalty factors. Hence, the correlations used to fit the data were two-degree polynomials in lubricant mass fraction and refrigerant mass flux.

Two forms of the $EF_{s'/s}$ or $PF_{s'/s}$ correlations were used to fit the smooth tube data:

$$EF_{s'/s} \; or \; PF_{s'/s} = a0 + a1(\omega_l) + a2(\omega_l G') + a3(\omega_l^2 G') + a4(\omega_l G'^2) + a5(\omega_l^2 G'^2) + \; a6(\omega_l^2) \tag{13}$$

$$ln\left(EF_{s'/s}\right) \; or \; ln\left(PF_{s'/s}\right) = b0 + b1(\omega_l) + b2(\omega_l G') + b3\left(\omega_l^2 G'\right) + b4(\omega_l G'^2) + b5\left(\omega_l^2 G'^2\right) + \; b6\left(\omega_l^2\right) \tag{14}$$

here is the nominal flowing lubricant mass fraction. For example, at a 5% lubricant concentration is 0.05. G' is the normalized mass flux given by

$$G' = \frac{G}{250} \tag{15}$$

where 250 is the average mass used during testing. Equations 13 and 14 are two-degreepolynomials in lubricant mass fraction with interaction terms that are functions of the normalized mass flux. Two forms were used because in some cases one equation type is a significantly better fit to the data than the other type. Explicit mass flux terms were not included in either correlation for the smooth tube because with no lubricant concentration the correlation should reduce to 1.0. If terms explicit in mass flux were included, the ratios could vary with mass flux at a 0% lubricant mass fraction causing an inherent bias in the model.

Equations 16 and 17 were used to fit $EF_{a'/s}$ and $PF_{a'/s}$ data for the micro-fin tube.

$$EF_{a'/s} \; or \; PF_{a'/s} = c0 + c1(\omega_l) + c2(\omega_l G') + c3(\omega_l^2 G') + c4(\omega_l G'^2) + c5(\omega_l^2 G'^2) + \; c6(\omega_l^2) \tag{16}$$

$$ln\left(EF_{a'/s}\right) \; or \; ln\left(PF_{a'/s}\right) = d0 + d1(\omega_l) + d2(\omega_l G') + d3\left(\omega_l^2 G'\right) + d4(\omega_l G'^2) + d5\left(\omega_l^2 G'^2\right) + \; d6\left(\omega_l^2\right) \tag{17}$$

where is the nominal flowing lubricant mass fraction and G' is the normalized mass flux given by Equation 15. Equations 16 and 17 are two-degree polynomials in both lubricant concentration and normalized mass flux. For the micro-fin tube, the $EF_{a'/s}$ and $PF_{a'/s}$ are expected to vary with mass flux at a 0% lubricant concentration, and therefore, explicit mass flux terms are included.

The final form of the correlation used to fit the heat transfer enhancement factors and pressure drop penalty factors for each lubricant mixture was a subset of the terms found in Equations 13,14,16 and 17. Specifically, the full model was evaluated for each data set with a statistical analysis package and the important terms were selected by maximizing an adjusted R-squared parameter. The adjusted R-squared parameter is a weighted R-squared parameter that includes a penalty factor for the number of terms in the model. The weighing is accomplished by dividing each sum of squares in the R-squared formula with the associated degrees of freedom.

When the adjusted R-squared parameter is maximized, the model includes the least number of terms that give a high R-squared fit.

Smooth Tube Correlations

The correlations presented in this section are least squares curve fits of the heat transfer enhancement factors ($EF_{s'/s}$) and the pressure drop penalty factors ($PF_{s'/s}$). The $EF_{s'/s}$ and $PF_{s'/s}$ ratios were formed from the least squares curve fits shown in Figures 2, 3, 7, and 8. Specifically, these ratios were formed by dividing the HFC-134a/lubricant mixture results in the smooth tube by pure HFC-134a results in the smooth tube at the same mass flux.

The $EF_{s'/s}$ and $PF_{s'/s}$ data for the two refrigerant-lubricant mixtures were fit to Equations 13 and 14. Tables 5 and 6 give the coefficients for both the $EF_{s'/s}$ and $PF_{s'/s}$ correlation. One important consideration for the smooth tube model is that when the lubricant concentration is zero the model should return a value of 1.0 for both the $PF_{s'/s}$ and $EF_{s'/s}$ ratio. The equations were selected to facilitate this requirement. Comparing the R-squared parameter in Tables 5 and 6 shows that the $EF_{s'/s}$ ratios were correlated slightly better by Equation 14 shown in Table 6. For the $PF_{s'/s}$ ratio, the two correlations have about the same R-squared value.

Micro-Fin Tube

Micro-fin tube heat transfer enhancement factors and pressure drop penalty factors are presented for both refrigerant/lubricant mixtures. The heat transfer enhancement factors ($EF_{a'/s}$) and pressure drop penalty factors ($PF_{a'/s}$) are formed by dividing the experimental results for refrigerant/lubricant mixtures in the micro-fin tube by the experimental results for the pure refrigerant in the smooth tube at the same mass flux.

The performance of the pure refrigerants in the micro-fin tube was not modeled specifically. However, the heat transfer enhancement factors ($EF_{a/s}$) or pressure drop penalty factors ($PF_{a/s}$) for the pure refrigerant can be obtained from the correlations. Specifically, the pure refrigerant performance in the micro-fin tube can be obtained by setting the nominal flowing lubricant mass fraction to zero in Equations 16 and 17. The only remaining terms are those for the mass flux.

The performance ratios $EF_{a'/a}$ or $PF_{a'/a}$ can also be obtained from the correlations. These ratios could be of interest to the designer who has micro-fin tube heat transfer coefficients and pressure drops for the pure refrigerant but wishes to estimate the effect of lubricant mass fraction on this data. The $EF_{a'/a}$ ratio is formed by dividing the $EF_{a'/s}$ ratio by the $EF_{a/s}$ ratio.

$$EF_{a'/a} = \frac{EF_{a'/s}}{EF_{a/s}} \tag{18}$$

$EF_{a/s}$ ratios are obtained as outlined in the previous paragraph. The $PF_{a'/a}$ ratio is obtained in a manner like that presented in Equation 18.

The least-squares estimation of the constants in Equations 16 and 17 for the $EF_{a'/s}$ ratio are shown in Tables 7 and 8. The $EF_{a'/s}$ ratios were fit well by Equation 16 shown in Table 7 with the lowest R-squared value being 0.89. Equation 17 shown in Table 8 is an equally good fit to the $EF_{a'/s}$ data with the lowest R-squared value being 0.88.

Table 5: Constants for Equation 13

	Heat Transfer $EF_{s'/s}$		Pressure Drop $PF_{s'/s}$	
	169 SUS ester	369 SUS ester	169 SUS ester	369 SUS ester
a0	1	1	1	1
a1	6.92	7.05	43.68	26.94
a2	0	0	24.01	17.23
a3	572.1	31.11	0	0
a4	0	0	0	0
a5	304.9	0	143.6	81.67
a6	0	63.55	341.8	0
R^2	0.83	0.89	0.96	0.96

Table 6: Constants for Equation 14

	Heat Transfer $EF_{s'/s}$		Pressure Drop $PF_{s'/s}$	
	169 SUS ester	369 SUS ester	169 SUS ester	369 SUS ester
b0	0	0	0	0
b1	9.66	7.1	37.54	24.41
b2	0	0	20.86	14.46
b3	753.6	49.49	296.2	0
b4	2.78	0	0	0
b5	449.3	0	0	92.97
b6	0	57.9	460.4	87.9
R^2	0.88	0.9	0.97	0.88

Table 7: Constants for Equation 16

	Heat Transfer $EF_{a'/s}$		Pressure Drop $PF_{a'/s}$	
	169 SUS ester	369 SUS ester	169 SUS ester	369 SUS ester
c0	2.69	2.29	1.31	1.28
c1	17.27	1.23	10.08	4.07
c2	1.43	0.99	0.22	0.15
c3	0	0.76	0	0
c4	0	0	0	0
c5	3.73	0	0	76.8
c6	0	0	0	177.5
c7	508.2	0	0	239.7
c8	0.39	0.26	0	0
R^2	0.89	0.89	0.65	0.88

Table 8: Constants for Equation 17

	Heat Transfer $EF_{a'/s}$		Pressure Drop $PF_{a'/s}$	
	169 SUS ester	369 SUS ester	169 SUS ester	369 SUS ester
d0	1.02	0.91	0.26	0.24
d1	10.42	1.67	7.3	2.46
d2	0.7	0.6	0.16	0.12
d3	0	1.68	0	0
d4	0	2.64	0	0
d5	1.87	0	0	6.09
d6	0	0	0	134
d7	298.3	1.99	0	164.8
d8	0.17	0.14	0	0
R^2	0.9	0.88	0.64	0.9

The $PF_{a'/s}$ ratio for both refrigerant/lubricant mixtures were also fit to Equations 16 and 17. The least squares estimates of the constants in Equation 16 are shown in Table 7 and those from Equation 17 in Table 8. Most of the refrigerant/lubricant mixture $PF_{a'/s}$ data were fit well with R-squared values of 0.85 or higher. The mixture of HFC-134a and the 169 ester lubricant was an exception, with an R-squared values of about 0.65.

CONCLUSIONS

In-tube heat transfer coefficients and pressure drops were reported for mixtures of HFC-134a and an ester lubricant in a micro-fin tube and a smooth tube. The ester lubricant was tested at viscosities of 169 SUS and 369 SUS over a 0% to 5% lubricant concentrations. The average heat transfer coefficients and pressure drops were measured in a 3.67-m-long (12 ft), 9.52-mm (3/8 in) outer diameter smooth tube and micro-fin tube over a mass flux range of 85 kg/m^2s (62,700 lb/ft^2 hr) to 375 kg/m^2 s (276,600 lb/ft^2 hr).

Heat transfer coefficients during evaporation were decreased by the addition of lubricant in both the micro-fin tube and smooth tube except at low lubricant concentrations of the 169 SUS lubricant. The micro-fin tube heat transfer coefficients were 100% higher than those for the smooth tube at a mass flux of 125 kg/m^2s (92,200 lb/ft^2 hr) and 50% higher at a mass flux of 375 kg/m^2s (276,00 lb/ft^2 hr). Pressure drops in both the smooth tube and micro-fin tube were increased with the addition of either viscosity lubricant. The micro-fin tube in general had 5% to 15% higher pressure drops than those for the smooth tube.

The design correlations presented for the heat transfer coefficients and pressure drops were a curve fit of ratios created from the experimental data. Specifically, ratios were formed by dividing the refrigerant-lubricant mixture results in both the smooth tube and micro-fin tube by the pure refrigerant results in the smooth tube at the same mass flux. The EF and PF ratios for the smooth tube and micro-fin tube were curve-fit as functions of lubricant mass fraction and refrigerant mass flux. The EF and PF correlations are used to modify pure refrigerant smooth tube data to predict the performance of refrigerant-lubricant mixtures in the smooth tube and micro-fin tube.

ACKNOWLEDGEMENTS

Support for this project was provided by ASHRAE Research Project RP-630. The guidance provided by the Sponsoring Technical Committee, TC 1.3, Heat Transfer and Fluid Flow, and the Project Monitoring Committee (Dr. Naim Azer, Mr. Keith Starner, and Dr. Lynn Schlager) are greatly appreciated.

NOMENCLATURE

a = Surface area
a0-a6 = Equation 13 constants
b0-b6 = Equation 14 constants
c0-c8 = Equation 15 constants
c_p = Specific heat
d0-d8 = Equation 16 constants
EF = Heat transfer enhancement factor
G = Mass flux
G' = Normalized mass flux
h = Heat transfer coefficient
H = Enthalpy
I = Current
i_{fg} = Enthalpy of vaporization
LMTD = Log-mean-temperature-difference
m = Mass flow rate
PF = Pressure drop penalty factor
Q = Heat transfer rate
T = Temperature
U = Over all heat transfer coefficient
V = Voltage
x = Quality

<u>Greek</u>

= Lubricant mass fraction
= Density

<u>Subscripts</u>

BL = Boiler
a = Pure refrigerant, micro-fin tube
a' = Refrigerant/lubricant, micro-fin tube
h = Pre-heater
I = Inlet
i = Inner surface
l = Lubricant
O = Outlet
o = Outer surface
r = Refrigerant
s = Pure refrigerant, smooth tube
s' = Refrigerant/lubricant, smooth tube
sat = Saturation

T = Test section
w = Water

REFERENCES

ASHRAE. 1984a. "ANSI/ASHRAE Standard 41.4-1984: Standard method for measurement of proportion of oil in liquid refrigerant." Atlanta, GA: American Society of Heating, Refrigerating and Air-Conditioning Engineers, Inc.,

ASHRAE. 1984b. "Lubricants in refrigerants." In *ASHRAE Handbook - 1984 Systems*. Atlanta GA: American Society of Heating, Refrigerating and Air-Conditioning Engineers, Inc.

Chaddock, J. B., and H. Brunemann. 1967. "Forced convection boiling of refrigerants in horizontal tubes-Phase 3." Durham, NC: Duke University School of Engineering, HL-113.

Eckels, S.J., T. B. Doerr, and M. B. Pate. 1994. "In-tube Heat transfer and Pressure Drop of HFC-134a and Ester Lubricant Mixtures in a smooth tube and a Micro-fin tube: Part II Condensation" *ASHRAE TRANSACTIONS*

Eckels, S.J., S. C. Zoz, and M. B. Pate. 1993. "Using solubility data for HFC-134a and ester lubricant mixtures to model an in-tube evaporator or condenser" *ASHRAE TRANSACTIONS* Vol. 99, part 2.

Eckels S.J., and M. B. Pate. 1991. "In-tube evaporation and condensation of refrigerant- lubricant mixtures of HFC-134a and CFC-12." *ASHRAE Transactions* Vol. 97, Part2, pp. 62-71.

Fukushima, T. and M. Kudou. 1990. "Heat transfer coefficients and pressure drops for forced convection boiling and condensation of HFC-134a." In: *Proceedings of the 1990: USNC/IIR-Purdue Refrigeration Conference* pp. 196-204.

Gungor, K. E., and R. H. S. Winterton. 1986. "A general correlation for flow boiling in tubes and annuli." *International Journal of Heat and Mass Transfer* Vol. 29, pp. 351-358.

Hambraeus, K. 1991. "Heat transfer coefficient during two-phase flow boiling of HFC-134a." *International Journal of Refrigeration* Vol. 14, pp. 357-362.

Jung, D. S., M. McLinden, R. Radermacher, and D. Didion. 1989. "A study of flow boiling heat transfer with refrigerant mixtures." *International Journal of Heat and Mass Transfer* Vol. 32, pp. 1751-1764.

Jensen, M. K., and D. L. Jackman. 1984. "Predictions of nucleate pool boiling heat transfer coefficients of refrigerant-oil mixtures" *Journal of Heat Transfer* Vol. 106, pp. 184-190.

Kandlikar, S. S. 1987. "A general correlation for saturated two-phase flow and boiling heat transfer inside horizontal and vertical tubes." ASME Winter Annual Meeting, Boston, MA, December 13-18. In: *Boiling and Condensation in Heat Transfer Equipment*, HTD-Vol. 85, pp. 9-19, New York, ASME.

Kline, S. J., and F. A. McClintock. 1953. "Describing uncertainties in single sample experiments." *Mechanical Engineering* Vol. 75, pp. 3-8.

Schlager, L.M. 1989. "Effect of oil on heat transfer and pressure drop inside augmented tubes during condensation and evaporation of refrigerants." Ph. D. dissertation, Iowa State University, Ames.

Schlager, L.M., M. B. Pate, and A. E. Bergles. 1987. "Evaporation and condensation of refrigerant-oil mixtures in a smooth tube and micro-fin tube." *ASHRAE Transactions* Vol. 93, pp. 293-316.

Shah, M. M. 1982. "Chart correlation for saturated boiling heat transfer: equations and further study." *ASHRAE Transactions* Vol. 88, pp. 66-86.
Torikoshi, K. and K. Kawabata. 1992. "Heat transfer and pressure drops characteristics of HFC-134a in a horizontal heat transfer tube" In: *Proceedings: 1992 International Refrigeration Conference - Energy Efficiency and New Refrigerants* Vol. 1, pp.167-176.

Table 5: Constants for Equation 13

	Heat Transfer $EF_{s'/s}$		Pressure Drop $PF_{s'/s}$	
	169 SUS ester	369 SUS ester	169 SUS ester	369 SUS ester
a0	1	1	1	1
a1	6.92	7.05	43.68	26.94
a2	0	0	24.01	17.23
a3	572.1	31.11	0	0
a4	0	0	0	0
a5	304.9	0	143.6	81.67
a6	0	63.55	341.8	0
R^2	0.83	0.89	0.96	0.96

Table 6: Constants for Equation 14

	Heat Transfer $EF_{s'/s}$		Pressure Drop $PF_{s'/s}$	
	169 SUS ester	369 SUS ester	169 SUS ester	369 SUS ester
b0	0	0	0	0
b1	9.66	7.1	37.54	24.41
b2	0	0	20.86	14.46
b3	753.6	49.49	296.2	0
b4	2.78	0	0	0
b5	449.3	0	0	92.97
b6	0	57.9	460.4	87.9
R^2	0.88	0.9	0.97	0.88

Table 7: Constants for Equation 17

	Heat Transfer $EF_{a'/s}$		Pressure Drop $PF_{a'/s}$	
	169 SUS ester	369 SUS ester	169 SUS ester	369 SUS ester
c0	2.69	2.29	1.31	1.28
c1	17.27	1.23	10.08	4.07
c2	1.43	0.99	0.22	0.15
c3	0	0.76	0	0
c4	0	0	0	0
c5	3.73	0	0	76.8
c6	0	0	0	177.5
c7	508.2	0	0	239.7
c8	0.39	0.26	0	0
R^2	0.89	0.89	0.65	0.88

Table 8: Constants for Equation 17

	Heat Transfer $EF_{a'/s}$		Pressure Drop $PF_{a'/s}$	
	169 SUS ester	369 SUS ester	169 SUS ester	369 SUS ester
d0	1.02	0.91	0.26	0.24
d1	10.42	1.67	7.3	2.46
d2	0.7	0.6	0.16	0.12
d3	0	1.68	0	0
d4	0	2.64	0	0
d5	1.87	0	0	6.09
d6	0	0	0	134
d7	298.3	1.99	0	164.8
d8	0.17	0.14	0	0
R^2	0.9	0.88	0.64	0.9